

**Final Technical Report**  
**On**  
**Studies on Green Polymeric Nanocomposites for Development of Insect**  
**Repellent Formulations**



Sponsored By

**DRL, Tezpur**

Sanction No. *Sanction letter NO. DRL/1047/TC dated 2<sup>nd</sup> March 2011*



*Submitted By*

**Professor Niranjan Karak**  
**Chemical Sciences Department**  
**TEZPUR UNIVERSITY**  
**Tezpur – 784028, Assam**  
**12<sup>th</sup> May 2014**

# CONTENTS

1. Objectives	4
2. Work done	5-6
3. Introduction	6-8
4. Experimental	8-13
5. Results and Discussions	13-36
6. Conclusion	37
7. References	38-39
8. Publications	39

*Project title:*

**“Studies on Green Polymeric Nanocomposites for Development of Insect Repellent Formulations”**

**Subject:** Chemical Sciences

**Name of PI:** Professor Nirranjan Karak

**Institution:** Tezpur University

**Duration of Project:** 3 Years

**Date of Initiation:** 1<sup>st</sup> April 2011

**R. Trained No. & Names: Research Fellow:** One and Ms. Sujata Pramanik

**Specific Application of the work**

To synthesize vegetable oil based hyperbranched polymeric nanocomposites for use as a matrix in insect repellent.

## **OBJECTIVES OF THE PROJECT**

- (i) To develop a nanocomposites system providing controlled release of the herbal insect repellent for use in vaporizing devices.
- (ii) To evaluate the efficacy of the nanocomposite repellent system at different temperature ranges.
- (iii) To develop a nanocomposites based paint additive incorporating the herbal insect repellent.
- (iv) To evaluate the efficacy of the insect repellent paint additive.
- (v) To carry out chemical and physical characterization of the nanocomposite systems.
- (vi) To develop a nanocomposite system providing controlled release of the herbal insect repellent for use in vaporizing devices.
- (vii) To evaluate the efficacy of the nanocomposite repellent system at different temperature ranges.
- (viii) To develop a nanocomposite based paint additive incorporating the herbal insect repellent.
- (ix) To evaluate the efficacy of the insect repellent paint additive.
- (x) To carry out chemical and physical characterization of the nanocomposite system.
- (xi) To study the performance characteristic of the prepared vegetable oil based poly(ester amide) (PEA)/PAni nanofiber-immobilized DRL herbal repellent formulation.
- (xii) To evaluate the insect repellent paint additive with antistatic properties.
- (xiii) To standardize and evaluate the above prepared formulation.

## WORK DONE

The objectives of the proposed project could be fulfilled by proper designing of the entire research works in different parts. The works done to fulfill the present proposed project are as follows.

1. A state-of-the-art literature survey including patents in the area of poly(ester amide) (PEA) resin, conducting polymers and nanocomposites were done.
2. The chemicals, glass-wares and equipment sanctioned in the project are procured and a research fellow was appointed.
3. Synthesis of vegetable oil based PEA resin and to characterize the same was successfully done.
4. Polyaniline nanofiber was prepared by interfacial polymerization technique.
5. Characterization of the prepared PANi nanofiber was done.
6. Characterization of the prepared vegetable oil based poly(ester amide)/PANi nanofiber nanocomposites was done.
7. Immobilization of the herbal repellent onto the nanocomposite system was done.
8. Study on controlled release of the herbal repellent at different ranges and preliminary development of formulation for use in vaporizing device was done.
9. Characterization of the prepared vegetable oil based PEA/PANi nanofiber nanocomposites was done.
10. Evaluation of the sheet resistance of the prepared nanocomposites was done.
11. Characterization of the essential oils (provided by DRL, Tezpur) from their mass spectral patterns and retention times in GC-MS was done.
12. Study of repellent action of the immobilized herbal repellent mixture (provided in varying weight percentages of 4:1, 3:2 and 1:1) in terms of median knockdown time and percent mortality of *Aedes albopictus* mosquitoes when exposed to insect repellent formulation was done.
13. Immobilization of DRL herbal repellent formulation (mixture of essential oils) onto montmorillonite (MMT) dispersed in methyl ester of the castor oil was done.
14. Study of interactions of the essential oil mixture immobilized onto the MMT dispersed in bio-based fatty ester and their antibacterial activity and biocompatibility was done.
15. Determination of the repellent potency of MMT immobilized-DRL herbal repellent formulation in terms of median knockdown time and percent mortality.
16. Optimization of the prepared nanocomposites and MMT immobilized-DRL herbal repellent formulation by monitoring the repellent action of the same.

## 1. INTRODUCTION

The usage of synthetic repellents to fray away the biting arthropods dates thousands of years ago. Amongst all haematophagous arthropods, the mosquitoes act as top vector for the infectious diseases-carriers [1]. The transmission of diseases like malaria, filariasis, Japanese encephalitis, dengue, yellow fever and so on is an issue of enormous concern in context to human lives [2]. However several species of primates anoint their pelage by rubbing with millipedes and various plant species including *Citrus spp.*, *Piper marginatum*, *Clematis dioica*, *Orthoporus dorsovittatus* and so on [3]. The burning of herbs like *Nigella sativa*, *Laurus nobilis*, *Ferula gummosa* and *Azadirachta indica* also aided in driving away the nuisance mosquitoes [3,4]. A number of repellents were screened and consequently some synthetic repellents were formulated. The research on repellents is particularly motivated by the low efficacy of the available formulations. Thus the exploration of bio-inspired strategy for the development of environmentally benign insecticide is of great interest among the researchers.

The employment of green technology, in the niche of preparative protocols of the insecticides urges us to switch to bio-based resources as the starting materials, use of non-toxic solvents, stabilizing template etc. In context to the concerns regarding public health, the synthetic mosquito repellents were replaced by the natural active ingredients from plant sources like essential oils of *Curcuma longa*, *Acorus calamus*, *Azadirachta indica*, *Syzygium aromaticum* etc [5]. The repellency property of *Curcuma aromatica* (CA) [6] and *Zanthoxylum limonella* (ZL) [7] are well documented in literature. However the synergistic effect of the mixture of both these essential oils (CA-ZL) has not been explored till date. The antimicrobial potency of the active repellent is another important aspect as the microbial metabolites helps attract the mosquitoes [3]. But these essential oil repellents are short-lived in their effectiveness, which constricts their practical utility [8]. In this milieu, the immobilization of the CA-ZL system proves to be apt strategy for the controlled release, consequently resulting in increased efficacy of the repellent formulation. The high surface-to-volume ratio of the nanomaterials favoring high binding and immobilization capacity is an important proposition in this regard. Thus the immobilization strategy for the conjugation of the active repellent onto the nanomaterials is being increasingly explored.

Nanotechnology holds the prospect for *avant-garde* applications in myriad of domain [9]. Porosity of the nanomaterials may also play a crucial role in the adsorption of the active repellents [10]. Amidst the nanomaterials, PAni nanofiber [11] and montmorillonite (MMT)

[12] are viewed to be a low cost, non-toxic, ecologically compatible and effective porous scaffold nanomaterial with high surface area instrumental for the immobilization of the active repellents. However the need for controlled release profile of the active repellent immobilized nanomaterials urges the use of an efficient matrix which can suffice the same. To this end, poly(ester amide) (PEA) resin forms a promising group of polymeric materials for the controlled release profile of the repellent from the system [13]. Streamlining research in various scientific domains in accordance to the dictates of green chemistry has instigated to use bio-based resources for the synthesis of polymers which imparts advantages like ample availability, versatility in structure and compositions, ease of handling and inherent biodegradability apart from their renewability [14]. Among the different types of traditional and non-traditional vegetable oils, non-edible castor oil, *Ricinus communis* is proved to be a unique feedstock for the synthesis of the polymeric materials because of its many advantages including the presence of a very high percentage (90-95%) of ricinoleic acid, a 12-hydroxy oleic acid [15]. In this vein, the synthesis of castor oil based PEA seems to be promising. Moreover harnessing the multifunctional roles of the coupled essential oils *via* immobilization onto methyl ester of castor oil (MECO) dispersed MMT for mosquito repellent applications also forms an interesting proposition in regard to the design of efficient benign solvent assisted repellent formulation. MECO is envisaged to play the twin role of green solvent and stabilizing template to assist in the controlled release of the essential oils from the system.

Thus the present investigation attempts to study the antistatic and repellent efficacy of the immobilized DRL herbal formulation (CA-ZL) onto the prepared castor oil based PEA/PAni nanofiber nanocomposites. The immobilization of CA-ZL (in varied weight percentages) onto the MMT dispersed in MECO is also evaluated to design another repellent formulation. The above two repellent formulations were optimized in terms of their repellent activity. The study also delved into the antibacterial and mosquito repellent activity of the repellent formulation together with the biocompatibility of the same.

## 2. EXPERIMENTAL

### 2.1 Materials

Aniline (Merck, India) was double-distilled under reduced pressure using zinc dust (S.D. Fine-Chem Ltd, India) and stored at 2-5 °C prior to use. Castor oil (Sigma Aldrich, India), diethanol amine (Merck, India), phthalic anhydride (Merck, India) and isophthalic acid (Sisco Research Laboratory Pvt. Ltd., India) were used after drying *in vacuo* at 50 °C for overnight. Maleic anhydride (Merck, Germany) was used after drying in a vacuum oven at 30 °C. The bisphenol-A-based epoxy resin (BPA, Araldite LY 250) (epoxy equivalent—180–190 g/equiv. and density 1.16 g/cc at 25 °C) and poly(amido amine) hardener (HY 840) Hindustan Ciba Geigy Ltd., Mumbai and were used as received. The solvents like benzene, tetrahydrofuran (THF) and dimethylacetamide (DMAc) were distilled before use. Ammonium peroxydisulfate and hydrochloric acid (HCl) were purchased from Merck, India and used as received. All other chemicals were of analytical grade. CA-ZL repellent mixture obtained from DRL, Tezpur were filtered using membrane filter before incorporation into the matrix. The bacterial cultures and peripheral blood mononucleated cell (PBMC) for the biocompatibility test were obtained from the department of Molecular Biology and Biotechnology, Tezpur University.

### 2.2 Synthesis of hyperbranched poly(ester amide)

#### 2.2.1. Preparation of methyl ester of castor oil (MECO)

Castor oil was transesterified by refluxing them with large excess of super dry methanol and in the presence of sodium methoxide as catalyst. MECO so formed was extracted using petroleum ether [16].

#### 2.2.2. Preparation of diethanol amide of castor oil

MECO and diethanol amine was reacted at 110-115°C for 4 h using 0.5 wt% sodium methoxide (with respect to the methyl ester) as the catalyst. The N,N'-bis(2-hydroxyethyl)castor oil amide (DEFA) was obtained in quantitative yield.

#### 2.2.3. Preparation of PEA resin



Hyperbranched poly(ester amide) (HBPEA) resin was synthesized *via*  $A_2+B_2+A'A_2$  approach. It is pertinent to mention that HBPEA was prepared instead of PEA owing to explore the advantages of the presence of multiple functional groups in the former. Briefly, the fatty amide of the oil served as an  $A_2$  monomer, maleic anhydride, phthalic anhydride and isophthalic acid as a  $B_2$  monomer and diethanol amine, an  $A'A_2$  monomer for the preparation of HBPEA. The polycondensation reaction was accomplished using 0.8 wt% sodium methoxide as the catalyst *via*  $A_2+B_2+A'A_2$  approach. The yield obtained in this process was about 75%.

### **2.3. Preparation of PANi nanofiber**

PAni nanofiber was prepared by interfacial polymerization using aniline as the monomer, ammonium peroxy sulphate as the oxidant and HCl as the dopant in the aqueous/organic biphasic system [11]. CA-ZL oil mixture provided by DRL was immobilized onto the prepared nanofiber using the green tool of sonication. Briefly, CA-ZL oil mixture was poured into the tetrahydrofuran dispersed nanofibers under ambient condition for 10 min and kept under air-tight container before further study.

### **2.4. Preparation of HBPEA/PAni immobilized nanocomposite system**

HBPEA/PAni immobilized nanocomposite system was then prepared by adding varying weight percentages of the CA-ZL immobilized PANi nanofibers to the pre-formed HBPEA at 60-70 °C. The prepared immobilized nanocomposite system was named as repellent formulation 1. The prepared nanocomposites was cured by using epoxy-poly(amido amine) curing system. The nanocomposite was mechanically mixed with bisphenol-A based epoxy (at 60:40 weight ratio) followed by sonication for 15 min and then hand mixing with 50% poly(amido amine) (weight with respect to epoxy resin). The mixtures were then cast on mild steel plates (150 mm × 50 mm × 1.60 mm) and glass plates (75 mm × 25 mm × 1.75 mm) under ambient conditions, degassed in vacuum dessicator and then baked in a furnace at a definite temperature for specified period of time.

### **2.5. Preparation of MMT dispersed in MECO**

CA-ZL repellent mixture was immobilized onto MMT dispersed in MECO (repellent formulation 2) using the green chemistry tool of sonication. The reaction vessel was maintained in 0 °C to prevent the escaping of the essential oils from the system. The MMT immobilized oil was subjected to centrifugation at 6000 rpm for 15 min post sonication. The collected mass was repeatedly washed thrice with petroleum ether.

## **2.6. Repellency test**

The DRL oil immobilized nanocomposite and MMT dispersed in MECO were tested using a standard test chamber in the Entomology department of DRL, Tezpur. A number of 50-60 adult female *Aedes albopictus* mosquitoes (2-5 days old, obtained from mosquito rearing facility of DRL, Tezpur) were released in to a repellent test chamber with the repellent formulations filled in a vaporizing device, separately. The device was plugged in to an electric socket and kept on for a period of 120 minutes inside the chamber, and the experiment was repeated with fresh mosquitoes. The number of mosquitoes knocked down was recorded and the median knockdown time (KT<sub>50</sub>) of the repellent against mosquitoes was also estimated.

## **2.7. Antibacterial activity**

The antibacterial activity (quantified in terms of minimum inhibitory concentration, MIC) against *Bacillus subtilis* MTCC441 (Gram +), *Staphylococcus aureus* MTCC373 (Gram +), *Mycobacterium smegmatis* ATCC14468 (acid fast +) and *Escherichia coli* DH5 $\alpha$  (Gram -) were cultured in respective broth and determined (post serial dilution of stock solution) as described by micro-well dilution method. The MIC of the dispersed MMT and the MMT immobilized samples was determined by micro-well dilution method [17]. The bacterial cells were cultured in the liquid growth medium of 96-well microtiter plate and inoculated with different concentrations of the sample. The growth of the cells was assessed after 20 h of incubation time period and the MIC value was noted.

## **2.8. Biocompatibility**

The biocompatibility of the formulation was accessed by the following cytotoxicity screening of PBMC by enzyme-based 3-(4,5-dimethylthiazol-2-yl)-2,5-diphenyltetrazolium

bromide (MTT) assay [18] using and trypan blue staining [19]. The various steps involved in this test are as follows.

#### *Isolation and culturing of PBMC*

The PBMC were separated from the goat blood by sedimentation technique (density gradient centrifugation) using histopaque. The blood was collected in sodium citrate and diluted in 1:1 ratio with phosphate buffer saline (PBS) at pH 7.4. Differential migration of different cells in the blood during centrifugation resulted in the separation of the same into different layers. The blood was then layered with a Pastuer pipette on histopaque in 3:2 ratios in a wide transparent centrifuge tube. The bottom layer contained histopaque-aggregated red blood cells, followed by a diffuse layer containing granulocytes and unbound histopaque with PBMC fraction sandwiched at the interface between the unbound histopaque and uppermost plasma/platelet layer. The interface was collected after centrifugation at 400×g for 15 min and transferred to serum free DMEM (Dulbecco's Modified Eagle Medium). The diluted cell suspension was subjected to multiple washes in 20 mL serum free media at 70×g for 10 min. The final pellet of PBMC was resuspended in 2 mL of serum free medium. The PBMC were cultured for 2 h in RPMI-1640 medium supplemented with 10% fetal calf serum, antibiotic Penicillin-Streptomycin-Neomycin solution and incubated in a humidified 95% O<sub>2</sub> with 5% CO<sub>2</sub> atmosphere at 37 °C. The non-adherent cells were removed by washing and the remaining adherent cells were cultured in the same media for above mentioned time period.

#### *Trypan blue exclusion assay*

The biocompatibility of the pristine and nanocomposite films was evaluated using mammalian blood derived PBMC. The in vitro assessment of cell membrane integrity and proliferation of the PBMC onto the prepared films was determined by trypan blue exclusion assay<sup>10</sup> by the following method. In this test, cells adhered onto the film surface were stained with 0.4% trypan blue solution in PBS (pH 7.4). The visual distinction between unstained viable cells and blue-stained nonviable cells was done using microscope at 20X magnification.

#### *MTT assay*

In the *in vitro* biocompatibility assay, PBMC at a density of  $1 \times 10^4$  cells/well were seeded onto 96-well microplates at 37 °C under 5% CO<sub>2</sub> in water-saturated atmosphere and allowed to grow for 2 h. The metabolic activity of the viable cells was determined by using colorimetric MTT assay.<sup>11</sup> Film disc of diameter ~4 mm was added into each microplate followed by incubation under the same conditions for 18 h. MTT was added to the seeded wells at different time intervals of 0, 1, 12, 24 and 48 h followed by 4 h incubation under the above conditions. The absorbance of the above cultured media was then recorded spectrophotometrically at 550 nm. The untreated cells were taken as the control and the experiments were performed in triplicates.

## 2.9. Instruments and Testing methods

Fourier transform infrared spectroscopy (FTIR) was used to record FTIR spectra of the samples by Impact 410, Nicolet, USA, using KBr pellets. The UV-visible spectroscopy spectra were recorded by UV-1700 PharmaSpec spectrophotometer from Shimadzu, Japan for PANi nanofiber and the immobilized systems. The wide-angle diffractograms of the fine powdered PANi samples were measured with a scanning rate of 0.05 min<sup>-1</sup> over a wide scanning angle of  $2\theta = 10-70^\circ$  using CuK<sub>α</sub> radiation by a Rigaku X-ray diffractometer (Miniflex, UK). Photoluminescence spectra of PANi nanofiber was acquired using a Perkin-Elmer Ls-55 fluorescence spectrometer. The dispersion and surface morphology of PANi nanofiber in the nanocomposites were investigated by using transmission electron microscope (TEM) JEOL 21X at the operating voltage of 200 kV. The UV-visible spectroscopy of the samples was taken using UV-1700 PharmaSpec spectrophotometer from Shimadzu. The immobilization of the oil onto the nanomaterials was done using an ultrasonic sonotrode under the following conditions: 60% amplitude and 0.5 cycles for a time period of 10 min. The sheet resistance of the thin films was measured by the standard four-probe technique with linear probe configuration (M/S Osaw Industrial Products, India) and the reported results were averaged over a set of three independent measurements. The thermal degradation was carried out by a Shimadzu, USA thermal analyzer, TGA 50, from 25 °C to 700 °C at nitrogen flow rate of 30 mL/min. The mechanical properties (as per the ASTM D 412-51 T) such as tensile strength and elongation at break were measured with the help of a universal testing machine (UTM) of model Zwick Z010 (Germany) with a 5 kN load cell and at 40 mm/min jaw separation speed. The gloss characteristic of the cured films was found out by a mini glossmeter (Sheen instrument Ltd, U.K) at an angle of incidence of 60°. The scratch

hardness test (ASTM D5178/1991) of the cured films was performed by a scratch hardness tester (Sheen instrument Ltd, U.K) moving at the speed of 6 mm/s. Impact resistance was determined by a impact tester (S.C. Dey Co., Kolkata) as per the standard falling weight (ball) method (ASTM D 1037). In this test (falling ball method) a weight of 850 g was allowed to fall on the film coated on a mild steel plate from minimum to maximum falling heights of 100 cm. The maximum height was taken as the impact resistance up to which the film was not damaged. The chemical resistance test was performed in different chemical media as per the ASTM D 543-67 procedure by taking weighted amount of cured thermosets in 250 mL beakers containing 100 mL of the individual chemical medium for specified period of time.

### **3. RESULTS AND DISCUSSION**

#### **3.1 Synthesis of HBPEA**

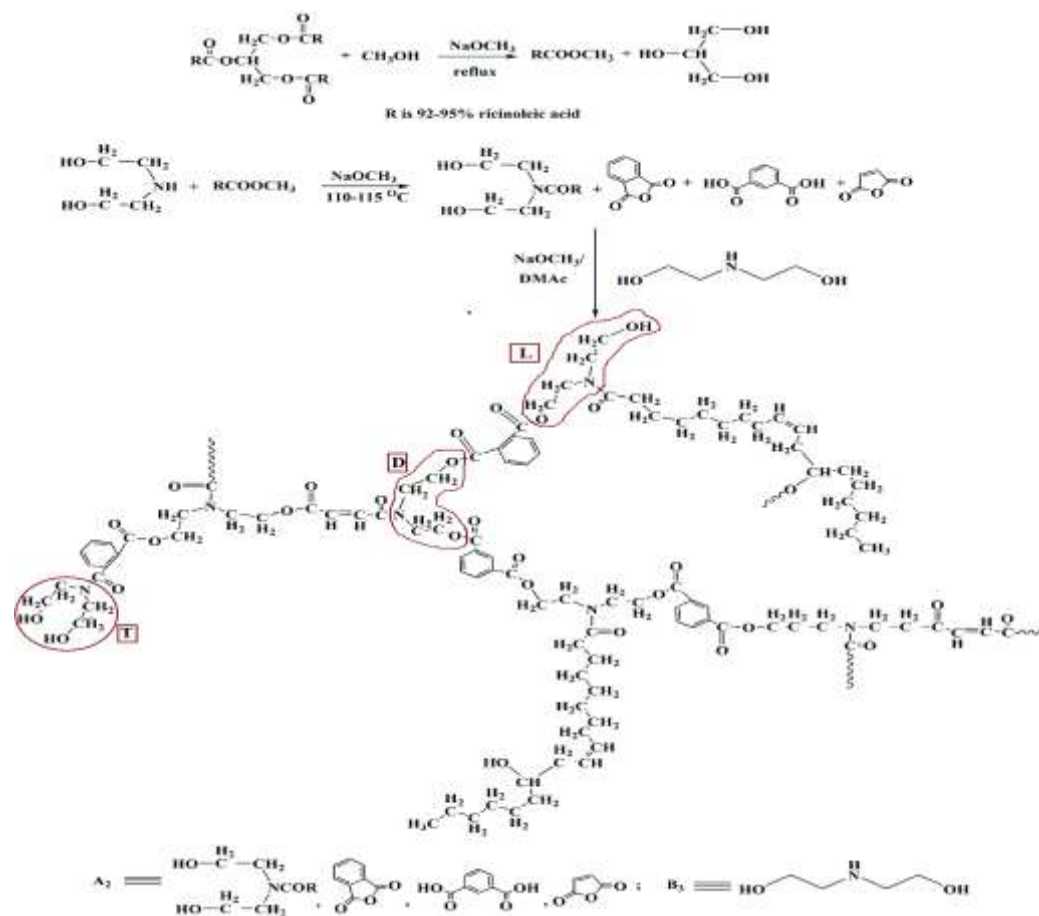
The polycondensation reaction of DEFA with the diacids (mole ratio 1:1.5) was carried out using the solution technique (Scheme 1). The use of sodium methoxide has advantages over the other conventional catalysts in enhancing the esterification rate. On one hand DEFA with the long hydrocarbon chain imparts flexibility into the structure whereas the presence of the aromatic moieties may result in good thermal stability of the thermoset.

The resinous HBPEA was converted to solid thermoset by the process of crosslinking through different types of possible chemical reactions with hydroxyl and epoxide group of epoxy resin and amino group of poly(amido amine) hardener with the hydroxyl and ester group of the resin. HBPEA resin was cured and the optimum temperature of baking was found to be 185 °C for the 2.5 h. Curing of the same at 150 °C required 10 h of time.

##### **3.1.1. Physical properties of HBPEA**

The physical properties of the resins like colour, acid value, saponification value, density etc. were determined and shown in Table 1. The moderate acid value of the resin supports its moderate reactivity for coating application. The saponification value of the resin supports the formation of a sufficient number of ester linkages in the resin which is further

confirmed by the FTIR spectra of the resin. The lower value of inherent viscosity indicates formation of hyperbranched branched structure of the resin.



*Scheme 1. Synthesis of HBPEA*

**Table 1:** Physical characterization of castor oil, MECO, DEFA and HBPEA

Property	Castor oil	MECO	DEFA	HBPEA
Color	Light yellow	Yellowish white	Yellowish brown	Light brown
Acid value (mg KOH/g)	0.32	-	-	2.55
Saponification value (mg KOH/g)	180	175	-	110
Specific gravity	0.95	0.90	0.92	0.98
Viscosity	<sup>a</sup> 950	0.7	0.65	0.09
(η <sub>inherent</sub> in 0.2% THF at 25 °C)				

### 3.1.2. FTIR spectra

The FTIR spectra of the castor oil, MECO, DEFA and HBPEA are shown in Fig. 1. The FTIR spectra indicate the formation of ester-amide linkages in the PEA resin. Further in the FTIR spectrum of the resin, the  $\text{-OH}$  absorption band appeared at  $3400\text{ cm}^{-1}$ , C-O (ester) at  $1177\text{ cm}^{-1}$ , C-N at  $1070\text{ cm}^{-1}$ ,  $\text{-CH}_2$  asymmetrical and symmetrical stretching at  $2926\text{ cm}^{-1}$  and  $2857\text{ cm}^{-1}$  respectively [13, 20-25].

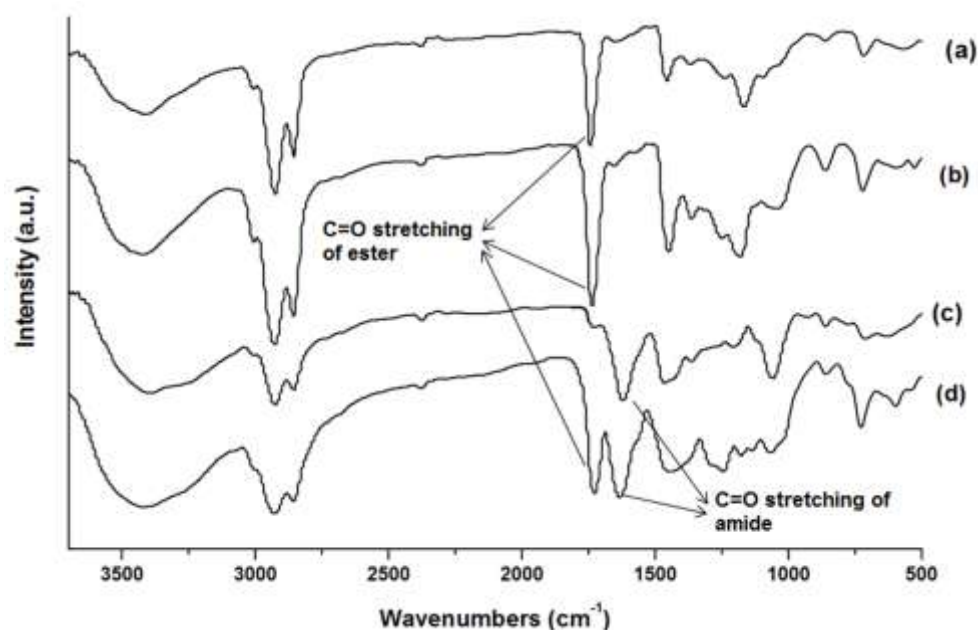


**Fig. 1.** FTIR spectra of (a) castor oil (b) MECO (c) DEFA and, (d) HBPEA.

### 3.1.3. NMR spectra

$^1\text{H}$  NMR of MECO, DEFA and HBPEA using  $\text{CDCl}_3$  are shown in Fig. 2a, 2b and 2c respectively. The singlet peak at around  $\delta = 0.85\text{--}0.89$  ppm occurs due to terminal methyl group of the fatty acid portion, whereas a broad singlet peak for the internal  $\text{-CH}_2$  group was observed at around  $1.31\text{--}1.25$  ppm [13]. The chemical shift value around  $1.22\text{--}1.45$  observed in the spectra is attributed to the beta ( $\beta$ )  $\text{-CH}_2$  proton of the  $\text{-OH}$  group, on the other hand the shift value for the  $\text{-CH}_2$  proton attached between the  $\text{-CH}$  and  $\text{-C=C-}$  was observed at around  $2.2$  ppm, in the spectra the shift observed at  $3.5$  ppm is ascribed to the  $\text{-CH}$  proton attached to the  $\text{-OH}$  group of ricinoleic acid, whereas the singlet peak at around  $5.4\text{--}5.5$  ppm and  $5.3$  ppm are assigned to the  $\text{-HC=CH-}$  and  $\text{O-H}$  protons of the fatty acid part, respectively [26]. The shift value observed at around  $2.7$  ppm and  $3.7$  ppm is assigned to the  $\text{-OH}$  and  $\text{-CH}_2$  protons attached to amide nitrogen of fatty amide of the oil (Fig. 2b). The

peaks at 2.63 ppm, 4.2 ppm, 7.4 ppm and 7.5 ppm are attributed due to the presence of maleic anhydride,  $-\text{CH}_2$  protons present between ester and amide groups, phthalic and isophthalic ring respectively in the polymeric structure of the resin.

$^{13}\text{C}$  NMR methyl ester, fatty amide of oil and poly(ester amide) resin are shown in Fig. 3a, 3b and 3c. The shift value ( $\delta$ ) at 14 ppm and 22.6-31.8 ppm are ascribed to the carbon of the  $-\text{CH}_3$  group and  $-\text{CH}_2$  of fatty acid chain respectively. The peaks at 125.4 ppm, 132.8 ppm, 174 ppm and 175 ppm are attributed to the aromatic carbon, ring carbon attached to  $-\text{COOCH}_2$  group of resin,  $-\text{C}=\text{O}$  of ester and amide groups respectively.

### 3.1.4. Coating performance

The moderate acid value of the resin supports its moderate reactivity for different binder applications. The saponification value of the resin endorses the formation of a sufficient number of ester linkages in the resin. The gloss values of the cured poly(ester amide) thermoset reflected the good compatibility of the poly(ester amide) with epoxy resin and the hardener, and the films have good dimensional stability and smooth surface texture. The high impact resistance of both thermoset reflected optimum crosslinking together with flexibility due to the presence of long hydrocarbon chain of the castor oil. Good scratch hardness of may be due to enhanced combined effect of strength and flexibility of the former than the latter. The long aliphatic chain of poly(amido amine) hardener imparted flexibility to the resin together with strength. The tensile strength of thermoset was found to be high. The performance characteristics of HBPEA thermoset are shown in Table 2.

**Table 2:** Performance of HBPEA thermoset

Physico-mechanical property	HBPEA
Curing time (h) at 150 °C	10
Scratch resistance (kg)	8
Impact resistance (cm)	100
Gloss at 60°	64
Tensile strength (MPa)	8.67
Elongation at break (%)	114



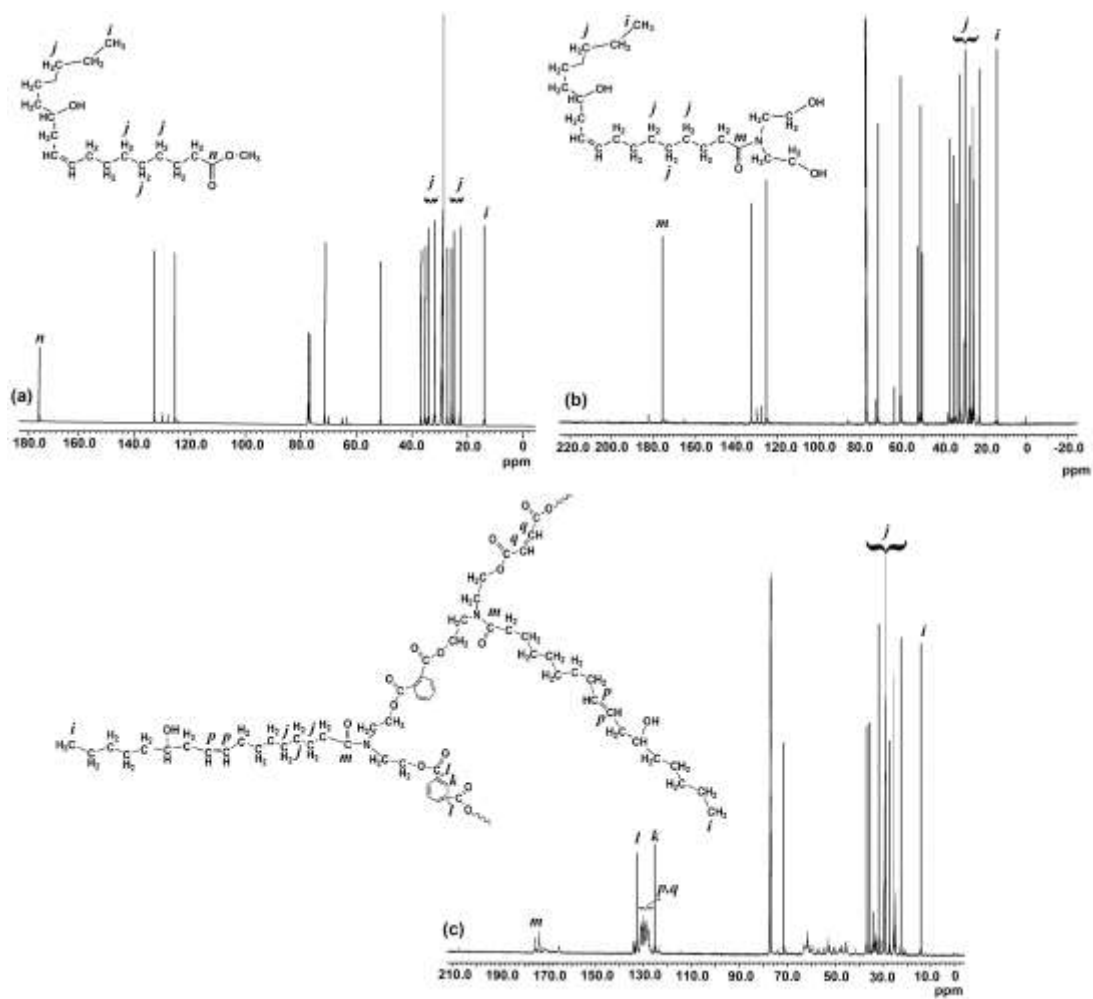
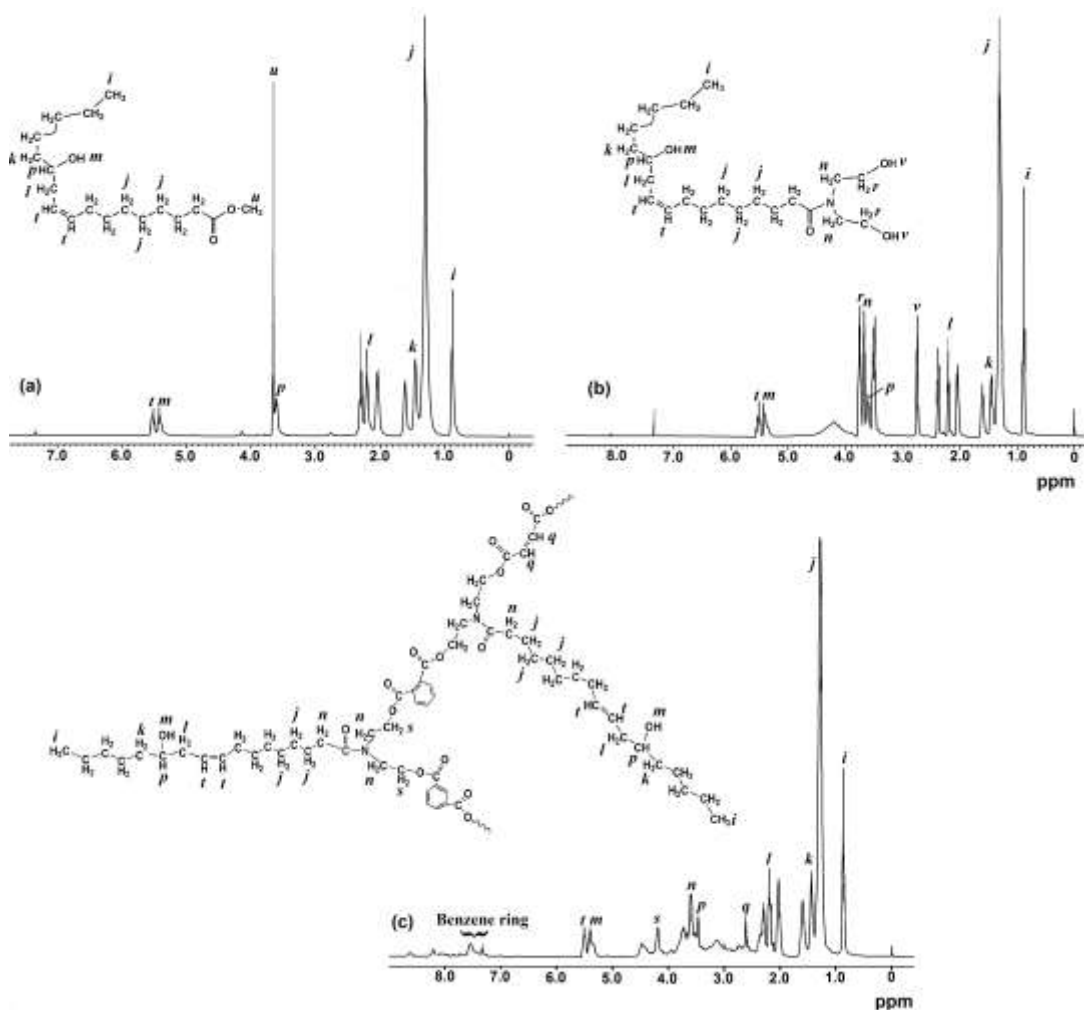


Fig. 2.  $^1\text{H}$  NMR spectra of (a) MECO, (b) DEFA and (c) HBPEA



**Fig. 3.**  $^{13}\text{C}$  NMR spectra of (a) MECO, (b) DEFA and (c) HBPEA.

### 3.1.5. Thermal behaviour

HBPEA thermoset showed a two step degradation pattern (Fig. 4) with initial degradation temperature (decomposition onset) around 250 °C. The first and second step degradation may be due to the presence of labile ester linkages and thermally stable aromatic moiety and amide linkages in the polymeric backbone respectively [27]. The TGA thermogram of HBPEA exhibited 50 wt% loss at 400 °C and a char residue of 3% at 700 °C. This is attributed to the strong interaction between the epoxy-poly(amido amine) system and HBPEA, which causes a trammel to the motion of the polymer chains.

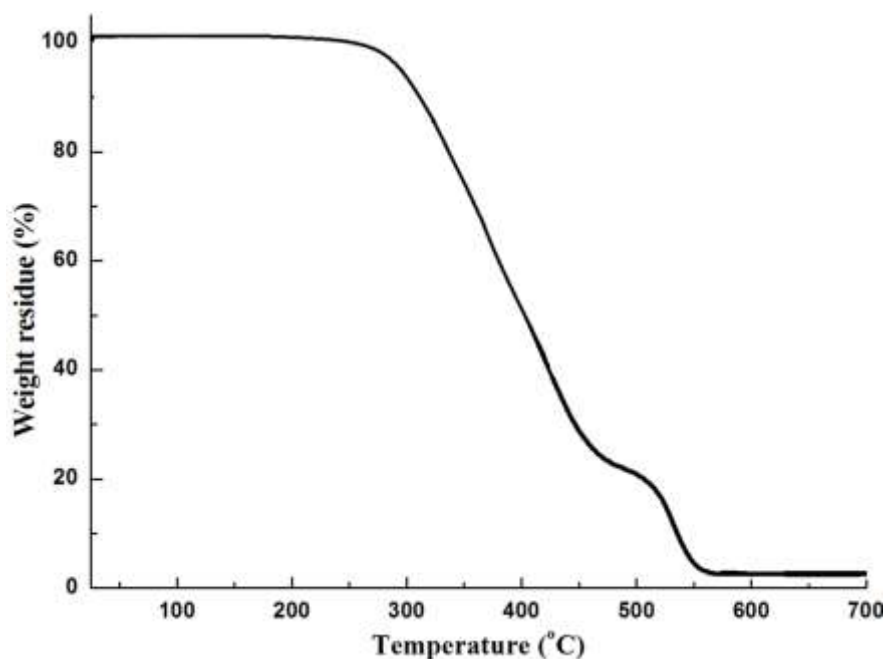


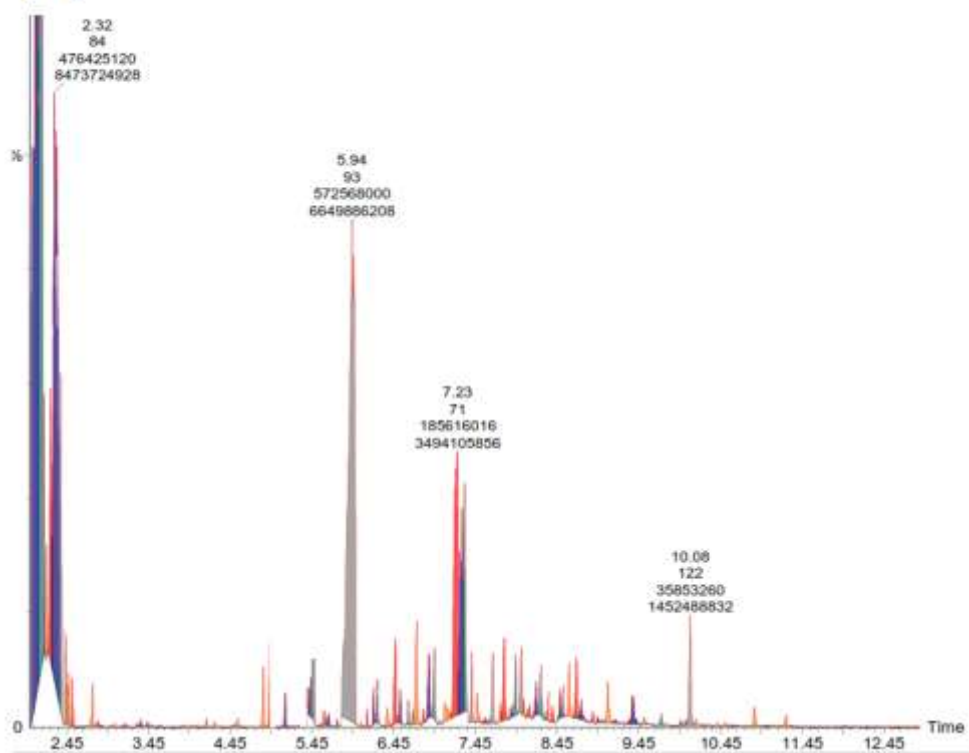
**Fig. 4.** TGA thermogram of HBPEA thermoset

### 3.2. GC-MS spectral analysis of CA-ZL essential oils (provided by DRL)

*Curcuma aromatic* (CA), an essential oil mainly consists of terpenoids and ketonic compounds. Amongst all, the bicyclic monoterpenoids like eucalyptol and camphor form 6.23 and 17.36% of the total components present. The oxygenated compounds constituting of 2-sec-butylcyclohexanone, 4,7-dimethyl-4,4a,5,6-tetrahydrocyclopenta[c]pyran-1,3-dione and tropolone make up the bulk components of the essential oil (76.40%) (Fig. 5(a)) [28].

The cyclic monoterpenes like D-limonene (45.07%) forms the major component of the mass spectral pattern of *Zanthoxylum limonella* (ZL). The spiro [4,5] decane and miscellaneous ketonic compounds like 2-(1-methylpropyl)cyclopentanone, 4,4,6-trimethylcyclohex-2-en-1-one and tropone make up rest of the components. The terpenoids like eucalyptol, camphor and D-limonene were reported to have mosquito repellent potency (Fig. 5(b)) [29].

(a)



(b)

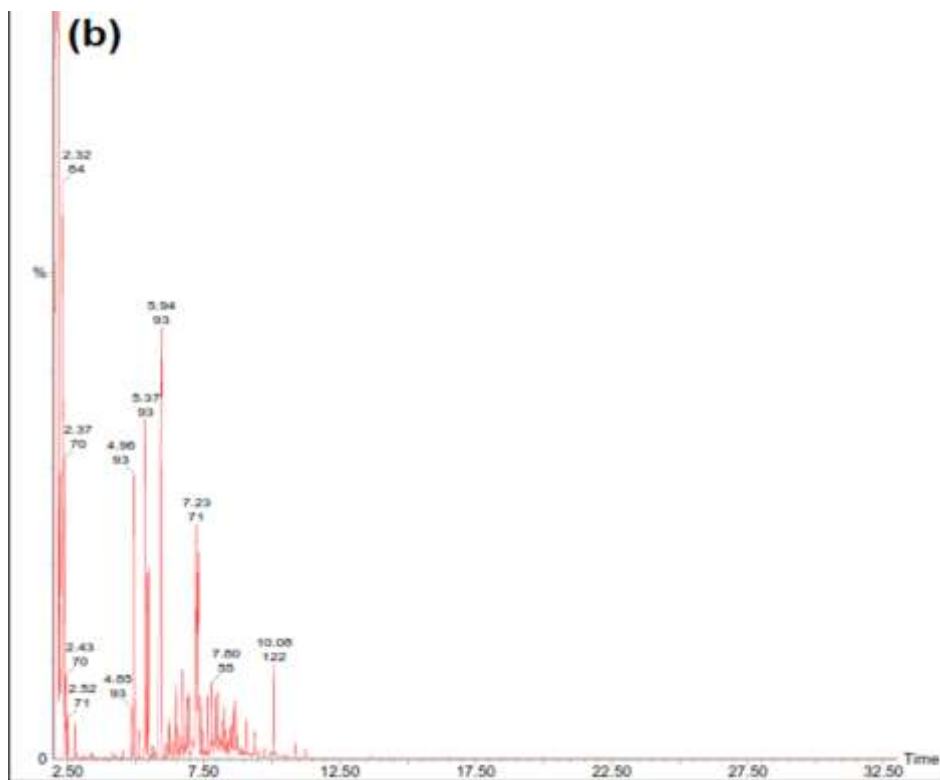


**Fig. 5.** GC-MS of (a) CA and, (b) ZL.

### 3.3. Characterization of the PANi nanofiber

The polymerization of aniline in different organic solvents by interfacial polymerization was monitored in terms of ‘induction time’ (the period from the addition of the two aqueous/organic biphasic systems to the beginning of the formation of PANi nanofibers at the interface of the two solvents) (summarized in Table 2). It is evident from Table 3 that the induction time is a function of the intermolecular interaction between the organic solvent and aniline (which in turn is dictated by the differences in their solubility parameters). Stronger interaction of aniline with the organic solvent (close solubility parameters) retards their interaction with APS in the aqueous phase containing HCl and hence results in longer “induction time”. In other words, smaller difference in the solubility parameter indicates similar internal energies and results greater interaction between aniline and organic phase, which consequently retards their interaction with the components of the aqueous phase. However although the difference in the solubility parameter are same in cases of 1-butanol and benzene, but the induction period of the former is more compared to the latter owing to the polar-polar and hydrogen bonding interactions of the former with the aniline monomer.

**Table 2:** Physical properties and Interactions of the organic solvents and induction time for the formation of PANi nanofiber

solvent	solubility parameter ( $\delta_s$ ) ( $\text{cal/cm}^3$ ) <sup>1/2</sup>	$\delta_a^* - \delta_s$ ( $\text{cal/cm}^3$ ) <sup>1/2</sup>	dielectric constant	dipole moment (D)	induction period (s)	quantum yield
CH <sub>2</sub> Cl <sub>2</sub>	9.7	0.6	9.1	1.60	90	0.24
C <sub>4</sub> H <sub>9</sub> OH	11.4	1.1	17.8	1.66	75	0.13
C <sub>6</sub> H <sub>6</sub>	9.2	1.1	2.3	0	60	0.11
CCl <sub>4</sub>	8.6	1.7	2.2	0	30	0.08

$\delta_a^*$ (solubility parameter of aniline) = 10.3 ( $\text{cal/cm}^3$ )<sup>1/2</sup>

#### 3.3.1. Morphology of the PANi nanofiber

The TEM micrographs (Fig. 6) exhibited the nanofibrillar morphology of PANi with average diameter around 25-30 nm.

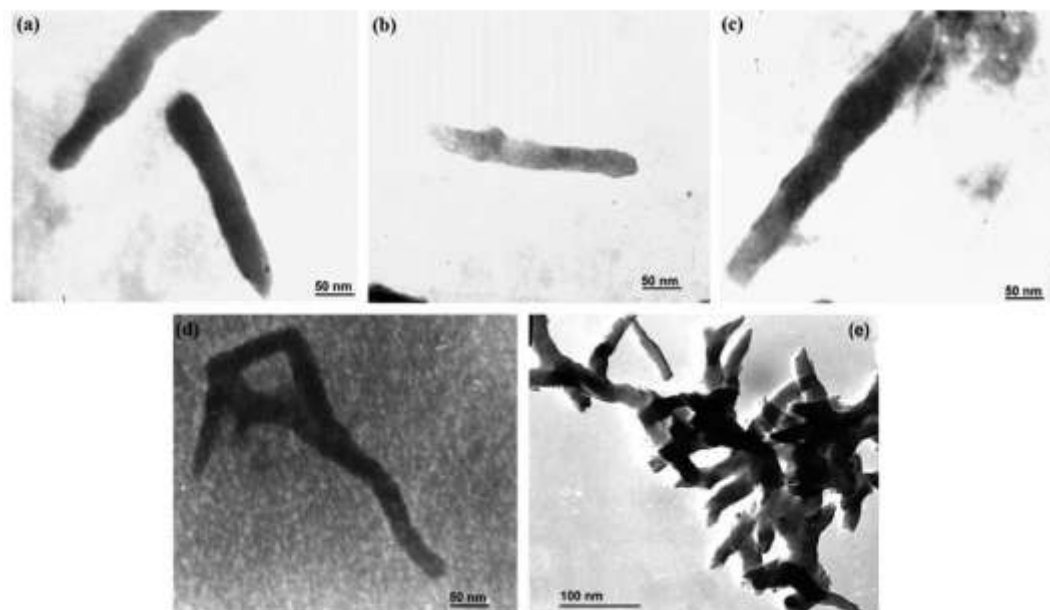


**Fig. 6.** TEM micrographs of PANi nanofibers

### 3.3.2. FTIR and current (I)-voltage (V) study of PANi nanofiber

The FTIR bands at around 3435, 1300 and 1150  $\text{cm}^{-1}$  are assigned to N-H, C-N and C=N stretching vibrations respectively [30]. The strong band at 1150  $\text{cm}^{-1}$  is ascribed as a measure of the degree of delocalization of electrons, a characteristic band of conducting PANi nanofiber. The characteristic bands at 1490 and 1576  $\text{cm}^{-1}$  are assigned to the benzenoid and quinoid rings, respectively and were deconvoluted computationally (Fig. 7). The strong absorption band at 1576  $\text{cm}^{-1}$  also corresponds to the coupling of the N-H bending and C-N stretching vibrations in PANi nanofiber. It was observed that greater the interaction (i.e. smaller difference in solubility parameter) of the solvent with the monomer, lesser is the benzenoid to quinoid ratio. The I-V characteristic curves of PANi nanofibers (Fig. 7 c) reveal that their conductivities increase with the decrease of interaction between the solvent and aniline. This is attributed to the increase in benzenoid to quinoid ratio,  $\pi$ -stacking of the PANi chains, and density of defect states with the decrease in interaction. The effective conjugation length of PANi nanofibers are thus strongly affected by its conformation because the degree of the p-orbital overlap in the extended p-bond is determined by the torsion angle of the backbone.

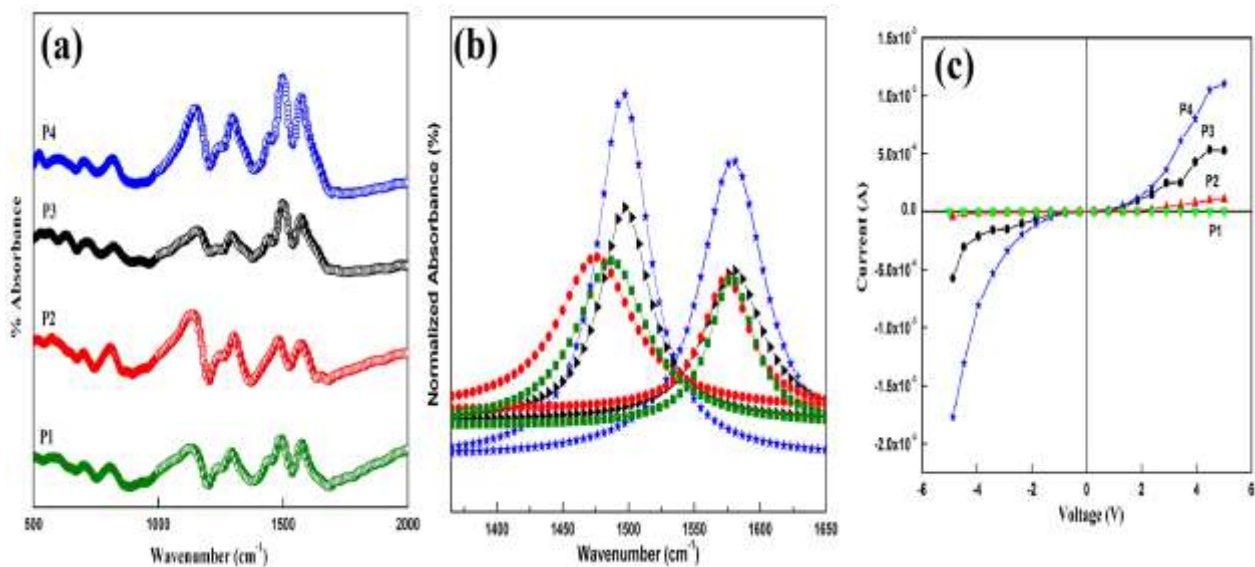


**Fig. 7.** (a) FTIR spectra of PANi nanofiber prepared using different solvents; (b) deconvolution of benzenoid-quinoid peaks; (c) I-V characteristic curve

### 3.3.3. Photoluminescence of PANi nanofiber

The photoluminescence (PL) spectra of different PANi samples are shown in Fig. 8. The nanofibers were excited at 220 nm and they showed luminescence in the blue region of the spectrum around 390 nm. It is observed that PL intensity is quenched with the increasing interaction of the solvent and aniline. This is indicative of the fact that the density of defect states decreases with the increase of interaction. This is further vouched by the characteristic I-V plots of the samples. The quantum yields of the PANi nanofibers have been found to decrease 0.24.

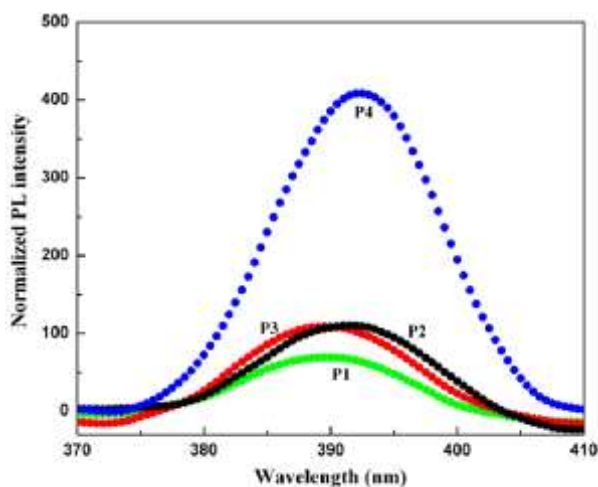
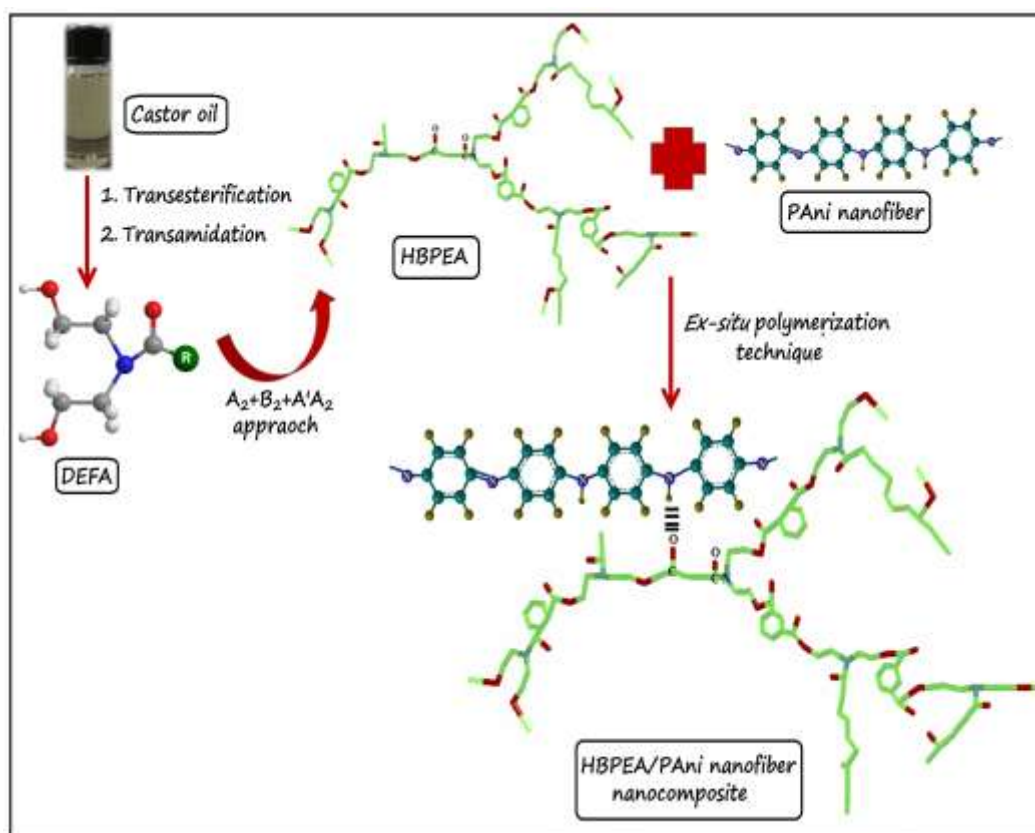


**Fig. 8.** (a) PL of PANi nanofibers

### 3.4. Preparation of castor oil based HBPEA/PAni nanofiber nanocomposite

The nanocomposites were prepared by an *ex-situ* polymerization technique and the preparative protocol is presented in Scheme 2. The nanoscale dispersion of the PAni nanofiber in the HBPEA matrix led to the effective interfacial interactions of the nanofiber with the polymer matrix, which subsequently confined the nanofiber in-between the polymer chains. The nano-confinement of the DRL herbal formulation in the HBPEA/PAni nanofiber nanocomposites helps in the control release of the same from the matrix.



*Scheme 2. Preparation of HBPEA/PAni nanofiber nanocomposite*

#### 3.4.1. Performance study

The performance characteristics of the epoxy-poly(amido amine) cured HBPEA/PAni nanofiber thermoset nanocomposites is tabulated in Table 3. The performance characteristics of the epoxy-poly(amido amine) cured HBPEA/PAni nanofiber thermoset nanocomposites effectively changed with the incorporation of varying amounts of PAni nanofiber (Table 3). The epoxy-poly(amido amine) cured polymer and its nanocomposites were baked at 150 °C for specified period of time. It was found that the curing time decreased with the increase of



the nanofiber content. This is attributed to the basic N-atom of PANi which acts as base and aids in the crosslinking reaction between HBPEA, epoxy and poly(amido amine) hardener. The increase in gloss with the increase of PANi nanofiber content in the nanocomposites indicated that the cured thermosets possessed good dimensional stability together with the smooth surface texture. The increment of scratch hardness of the nanocomposite thermosets with nanofiber content is due to the enhanced synergism of strength and flexibility of the polymeric chains. The high impact resistance of the thermosets reflected optimum crosslinking together with flexibility of the long hydrocarbon fatty amide chains.

The inclusion of the nanofiber into the HBPEA matrix resulted in the improvement the mechanical properties due to nano-reinforcing effect. The mechanical property of a nanomaterial-reinforced polymer depends on several parameters such as distribution and orientation, aspect ratio, domain size, shape and degree of compatibility of the nanomaterial with the polymer matrix. The efficiency of transferring of stress between the PANi nanofiber and HBPEA matrix is the prominent factor in improving the mechanical properties of the nanocomposites. The pristine HBPEA has a tensile strength of 7.2 MPa while it increases from 7.89 to 10.5 MPa with the increase of the PANi incorporation into the polymer matrix from 5 to 10 wt%. However the increment in the tensile strength even at 12.5 wt% was not so significant may be due to the agglomeration of the nanofiber (as evident from the TEM studies). The improvement in the mechanical properties of the nanocomposites compared to the pristine polymer is attributed to the interfacial bonding between the resin and the PANi nanofiber. The decrease of elongation at break (EB) of the thermosets with the nanofiber content is due to the decrease in molecular mobility of the polymer chains (Table 3). The good chemical resistance of the nanocomposite thermosets, particularly the alkali resistance is attributed to the presence of amide moiety and PANi nanofiber which aid in adequate amount of crosslinking in the thermosets (Table 4).

### **3.4.2. FTIR study**

The FTIR spectra of HBPEA and HBPEA/PANi nanofiber are shown in Fig. 9. The characteristic bands of HBPEA corresponding to  $\text{-C=O}$  appeared at  $1730\text{ cm}^{-1}$ , amide group at  $1632\text{ cm}^{-1}$  and hydrogen bonded  $\text{-OH}$  stretching at  $3422\text{ cm}^{-1}$  respectively. The characteristic peaks of PANi nanofiber shifted to  $1416$  and  $1506\text{ cm}^{-1}$  in the nanocomposites, which is attributed due to the interaction of the same with the pristine polymer. It was

observed that the absorbance band of ester moiety and amide shifted upon formation of the nanocomposite system, indicative of the interaction of the polymer with the nanofiber.

**Table 3:** Performance of HBPEA/PAni nanofiber nanocomposite

physico-mechanical property	HBPEAP5	HBPEAP7.5	HBPEAP10	HBPEAP12.5
curing time (h)	3.5	3.2	2.85	2.6
gel fraction (%)	79	79.8	81	81.2
scratch hardness (kg)	9	9.5	10	10
impact resistance (cm)	100	100	100	100
gloss at 60°	93	93.5	95	95.2
tensile strength (MPa)	7.89	8.4	10.5	12.25
elongation at break (%)	84.73	79.52	74.23	70.29

**Table 4:** Chemical resistance of HBPEA/PAni nanofiber nanocomposite

Type of medium	Weight change (g)				
	HBPEA	HBPEAP5	HBPEAP7.5	HBPEAP10	HBPEAP12.5
Water	$2.3 \times 10^{-2}$	$2.1 \times 10^{-2}$	$2.1 \times 10^{-2}$	$1.5 \times 10^{-3}$	$1.4 \times 10^{-2}$
5% aq. HCl	$3.2 \times 10^{-2}$	$2.6 \times 10^{-2}$	$2.4 \times 10^{-3}$	$2.3 \times 10^{-3}$	$2.3 \times 10^{-3}$
10% aq. NaCl	$1.3 \times 10^{-2}$	$1.0 \times 10^{-2}$	$1.1 \times 10^{-2}$	$1.1 \times 10^{-2}$	$1.2 \times 10^{-2}$
3% aq. NaOH	$1.2 \times 10^{-2}$	$1.2 \times 10^{-2}$	$1.1 \times 10^{-3}$	$0.7 \times 10^{-3}$	$0.7 \times 10^{-3}$

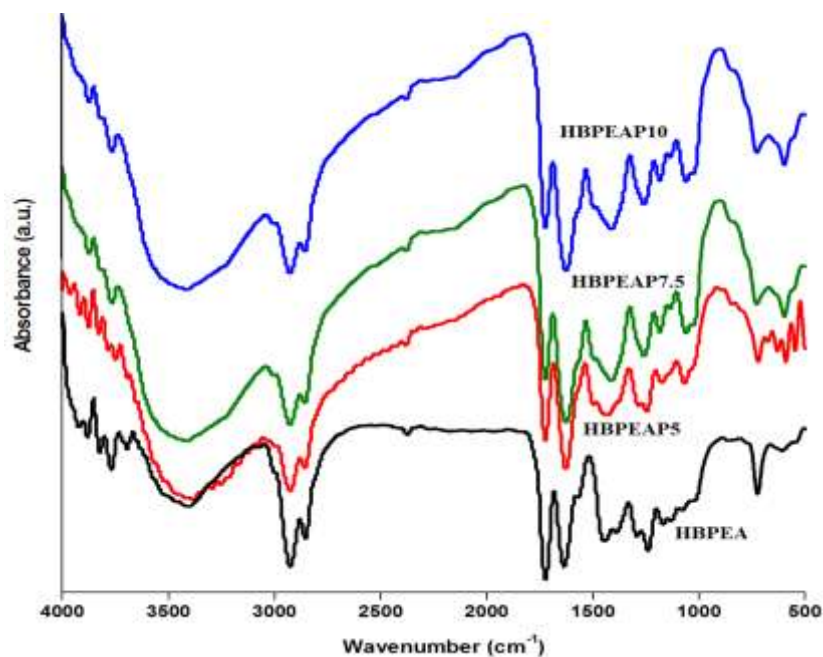


**Fig. 9.** FTIR spectra of HBPEA and HBPEA/PAni nanofiber nanocomposites

### 3.4.3. TEM study

Fig 10(a) and 10(b) shows the dispersion scenario of the PAni nanofiber in HBPEA matrix. HBPEA thermoset (Fig 8a) exhibited uniform surface morphology. The incorporation of PAni nanofiber in HBPEA matrix showed the connectivity between the nanofiber within the polymer matrix.

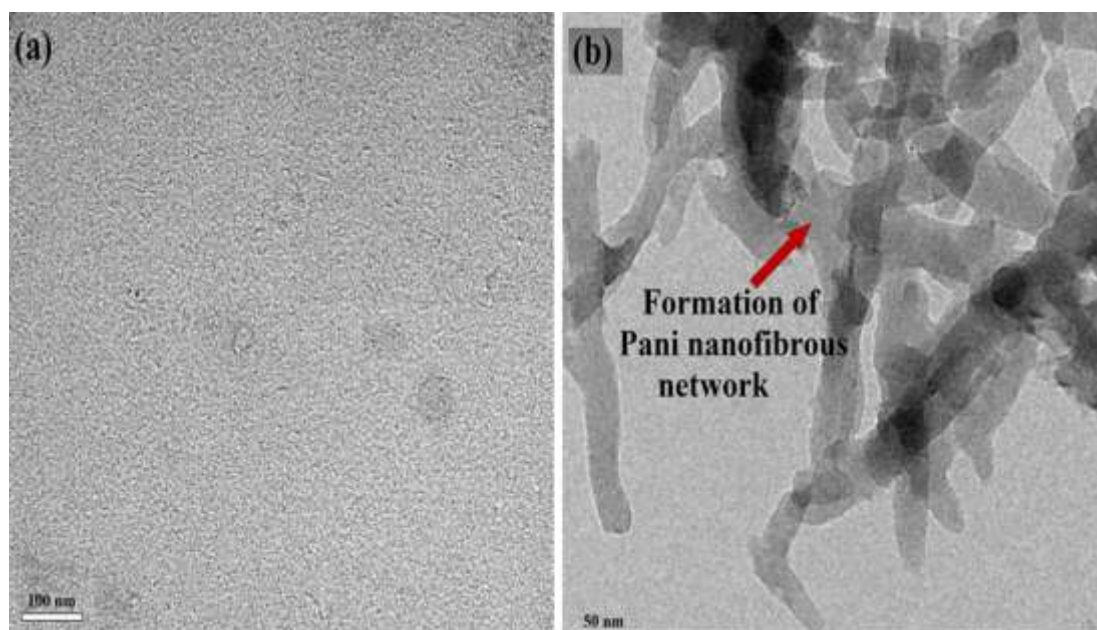


**Fig. 10.** TEM micrographs of (a) HBPEA and, (b) HBPEA/PAni nanofiber nanocomposite

### 3.5. Characterization of immobilization of repellent formulation 1

#### 3.5.1. UV-Visible study

The UV-visible spectra of PANi nanofiber, DRL herbal formulation and DRL herbal formulation-immobilized PANi nanofiber in tetrahydrofuran are shown in Fig. 11. The PANi nanofiber showed characteristic band at around 266 nm, corresponding to  $\pi$ - $\pi^*$  transition and a band centered at around 379 nm, corresponding to polaron- $\pi^*$  transition. The DRL herbal formulation showed an absorbance at around 265 nm. The DRL herbal formulation-immobilized PANi nanofiber showed bands at around 263 nm and 379 nm. The band at 263 nm indicates the interaction between the PANi nanofiber and the herbal formulation.

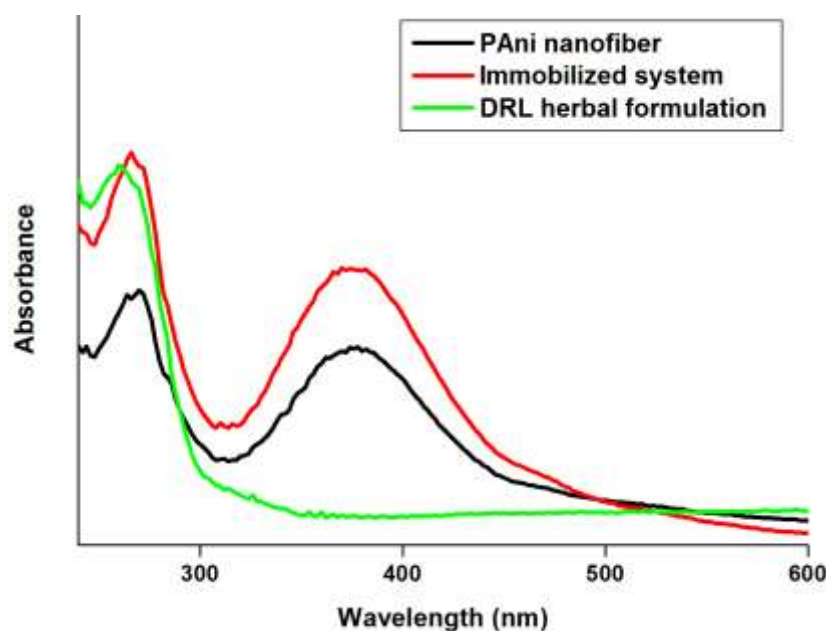


**Fig. 11.** *UV-Visible spectra of the PANi nanofiber, DRL herbal formulation and Immobilized system at room temperature*

#### 3.5.2. FTIR study

The FTIR spectra of DRL herbal formulation and repellent formulation 1 are shown in Fig. 11. The DRL herbal formulation exhibited bands at around 2971, 1764 and 1683  $\text{cm}^{-1}$  attributed to the presence of menthone-menthol, lactones and pulegone respectively. Further the bands at 1571, 1440, 1379, 993-760  $\text{cm}^{-1}$  confirmed the presence of menthofuran and a number of terpenes including limonene and cineole. The bands at 1257 and 1065  $\text{cm}^{-1}$  signified the presence of linalyl acetate and fenchyl alcohol respectively, which were in lines

with the as literature reports. The FTIR spectrum of the repellent formulation 1 showed the presence of almost all the peaks of the herbal formulation. Thus it can be inferred that the PANi nanofiber were efficiently immobilized with the functional moieties of the herbal formulation.

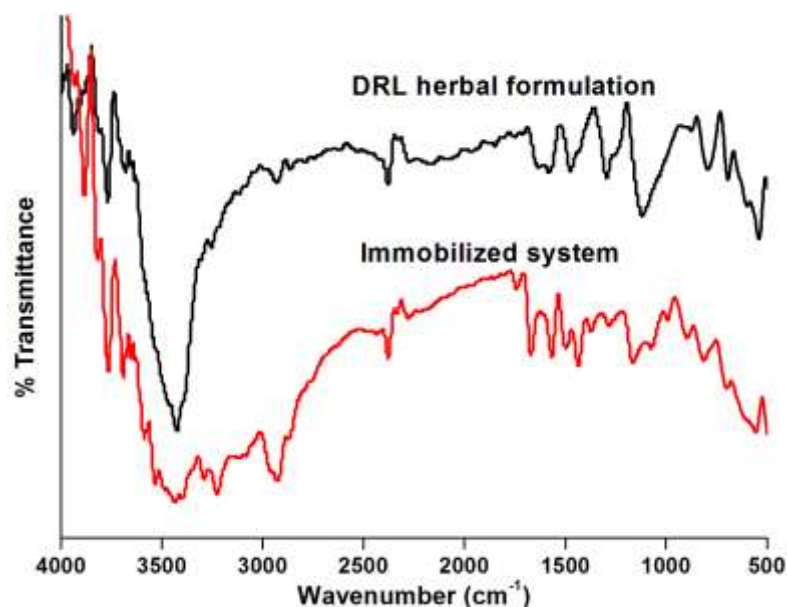


**Fig. 12.** FTIR spectra of DRL herbal formulation and Immobilized system

### 3.5.3. Release profile at different temperatures

The immobilization of DRL herbal formulation onto the PANi nanofiber in 1:1 (w/w) ratio was carried out by mixing the two using magnetic stirrer followed by sonication for 15 min in ice-cold condition. The immobilized system was washed several times with methanol to remove the free PANi nanofiber. The supernatant was checked using UV-Visible spectroscopy to find out the amount of washed out contents from the immobilized system. It was found that the supernatant contained less than 10 wt% DRL herbal formulation, which indicated the efficiency of immobilization process. Further the efficiency of the immobilized system was checked at different temperatures *viz.*, 30, 40 and 50 °C. It was observed that the UV-visible absorbance peak at 379 nm remained intact with no change in the intensity, while the peak at around 263 nm changed as a function of time and temperature. The magnitude of intensity decreased with increasing time and temperature owing to the release of the immobilized DRL herbal formulation. It can thus be inferred from Fig. 13 that the release profile of the immobilized system is in parallel lines with the increasing time and temperature.

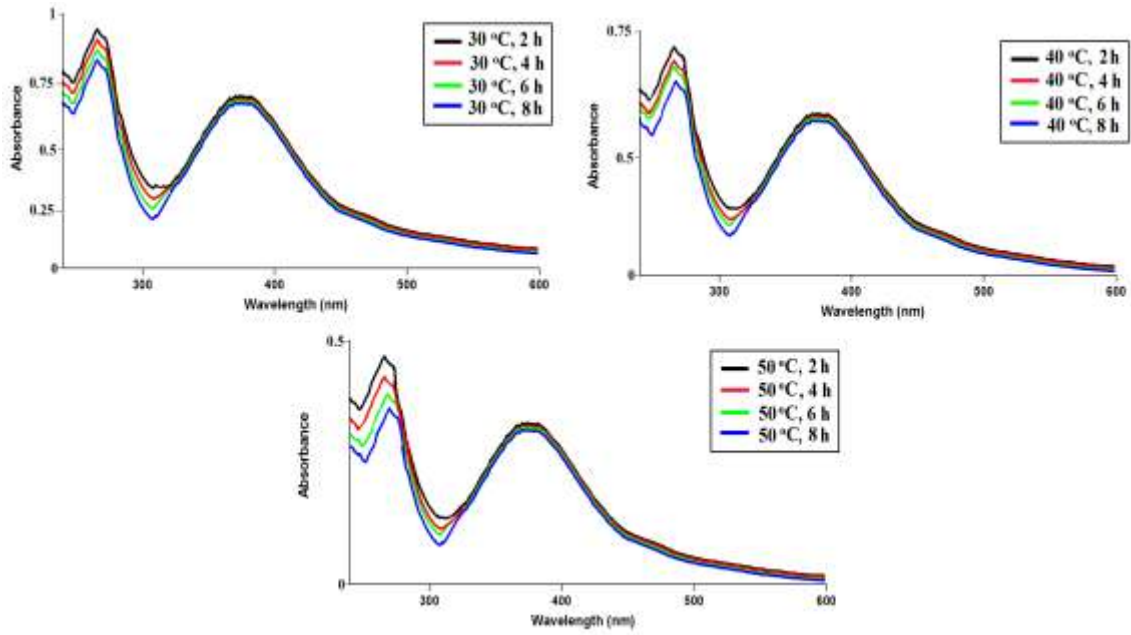


**Fig. 13.** Study of release profile of the immobilized system at different temperatures and time

### 3.5.4. Sheet resistance study

The variations of sheet resistance of the pristine and immobilized nanocomposite systems with PANi nanofiber content are shown in Fig. 14. The incorporation of PANi nanofiber with varying weight percentages from 5 to 12.5 led to the formation of electrically conductive networks (as evident from the magnitude of sheet resistances of the nanocomposites).

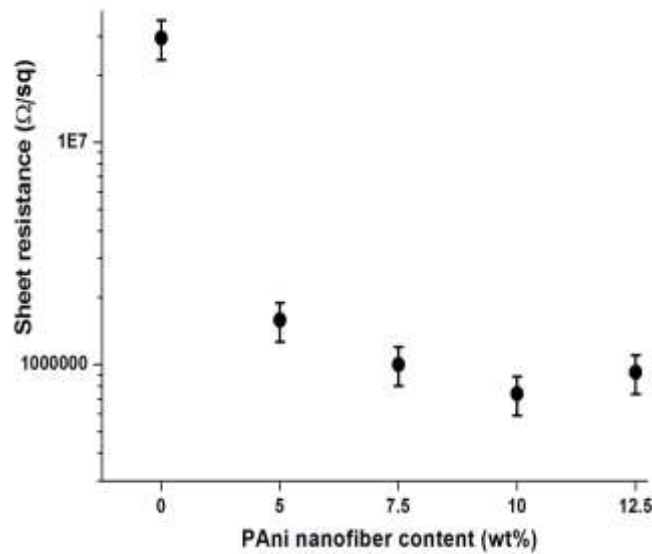


**Fig. 14.** Sheet resistance of the nanocomposites

### **3.5.5. Mosquito repellency activity of the repellent formulation 1**

The median knockdown time of the DRL oil immobilized nanocomposite system was found to be 91.3 min, indicating pronounced knockdown efficacy against the mosquitoes. However, the knockdown efficacies of the compositions were found to be much lower than that of commercially available vaporizers.

### **3.6. Physico-chemical attributes of the repellent formulation 2**

The FTIR spectra of MECO, MMT dispersed in MECO, ZL-CA oil extract and the immobilized system are shown in Fig. 15. The CA and ZL oil extracts exhibit C-H and C=O stretching at around 2940 and 1741  $\text{cm}^{-1}$  respectively. The peak at around 1670  $\text{cm}^{-1}$  is attributed to stretching frequency of the C=O group attached to the seven-membered ring of camphor and tropolone. The absorption peak at 1442  $\text{cm}^{-1}$  appears due to the C=C stretching in tropolone. The ZL-CA oil mixture showed similar bands as the individual oil extracts. The sharp absorption band observed at around 1736  $\text{cm}^{-1}$  (Fig. 15(b)) justified the formation of the ester linkages in the methyl ester of the oil. The MMT dispersed in methyl ester of the oil exhibited Si-O-Al and Si-O-Si characteristic stretching vibrational band of MMT at 528 and 1435  $\text{cm}^{-1}$  respectively together with the ester band. The immobilized system exhibited all the signature bands for MMT dispersed in the methyl ester of the oil. The formation of no new absorption band in the immobilized system infers that the immobilization is a physical adsorption process of the oil mixture onto the active surface of MMT. This adsorption process without forming any new chemical bonds indeed aids in the ease of the release profile of the immobilized oil mixture.

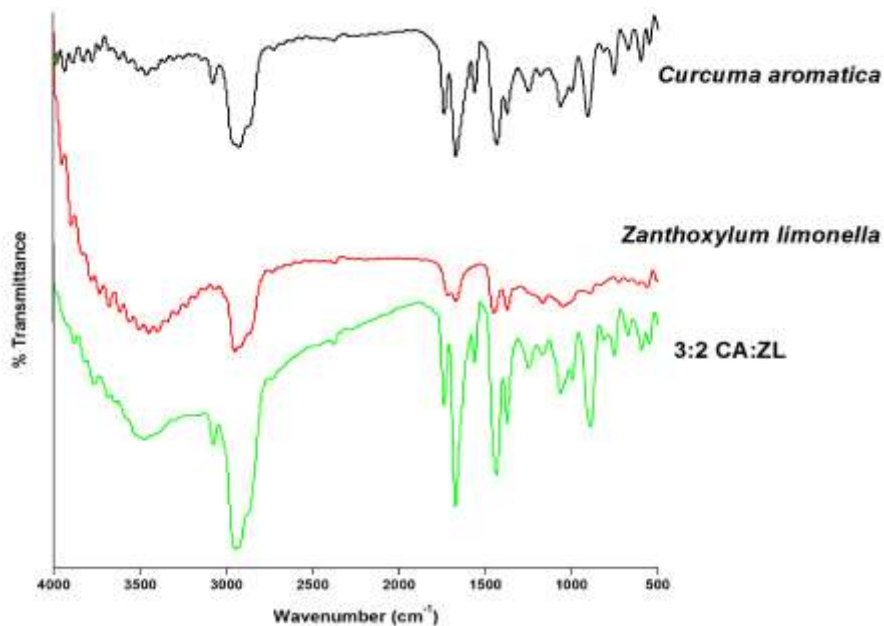


**Fig. 15.** FTIR of repellent formulation 2.

### 3.6.1. TEM study

The distribution of nanoplatelets of MMT in dispersed in MECO is evidenced from the HRTEM micrographs (Fig. 16). The images with a scale bar of 100 and 10 nm showed that the repellent formulation 2 exhibited a uniform distribution of the nanoplatelets within the MECO. This may be attributed to the presence of MECO and essential oils which aided in the modification of MMT and thereby causing their uniform dispersion in the benign solvent of MECO.

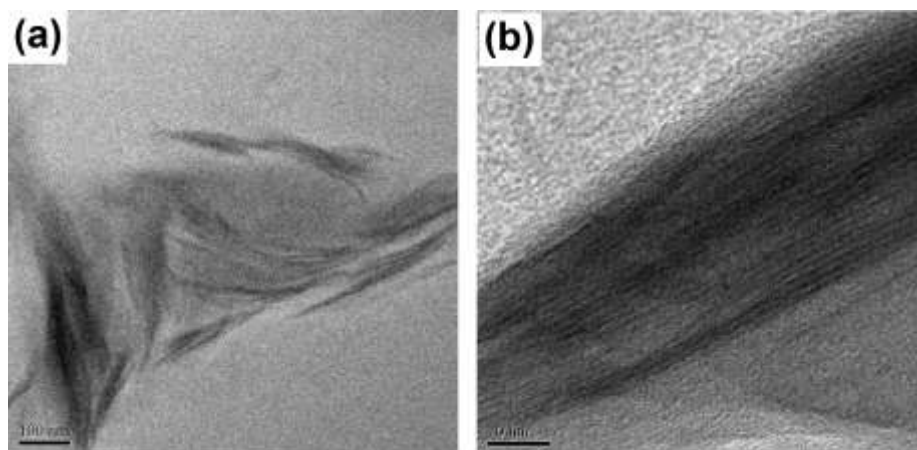


**Fig. 16.** TEM of the nanoplatelets of repellent formulation 2.



### **3.6.2. Mosquito repellency activity**

The median knockdown time ( $KT_{50}$ ) the 3:2 ratio containing CA and ZL essential oils mixture immobilized MMT dispersed in methyl ester of the castor oil was found to be provided 74.5 min. Mixing the two essential oils in other different compositions like 4:1 and 1:1 ratio and immobilizing the same onto the MMT dispersed in methyl ester of the castor oil gave  $KT_{50}$  of 88.7 and 101.5 min respectively, indicating that the 3: 2 ratio of the two essential oils is the ideal choice for incorporating into the matrix. Further the percent mortality of the 3:2 immobilized repellent formulation 2 was found to be 85.5%, in contrast to 78.7 and 82.2 for 4:1 and 1:1 immobilized repellent compositions.

Moreover the difference in fecundity and egg hatching between the repellent exposed and non-exposed mosquitoes were not found to be significant. This showed that the exposure to the repellent do not adversely affect mosquito fecundity.

### **3.6.3. Antimicrobial activity**

The antibacterial activity of the MMT dispersed in MECO, ZL-CA oil extract and the repellent formulation 2 were accessed by determining their MIC values (Fig. 17). It was observed from Fig. 17 that the MMT dispersed in the methyl ester of the oil exhibited almost no antibacterial activity. The ZL-CA oil extract and the immobilized system exhibited potent antibacterial efficacy with MIC value although less as compared to that of the antibiotics used as the control.

### **3.6.3. Biocompatibility**

The PBMC-matrix adhesion was evident from the Fig. 18(a). It was observed that the repellent formulation 2 supported the cell growth. The biocompatibility of the same with PBMC was further examined in terms of the former's effect on the latter's proliferation by the colorimetric MTT assay. The spectroscopic measurement of the solubilized formazan crystals (an indirect measurement of the activity of the mitochondrial dehydrogenase) in MTT assay is directly related to the number of viable cells. Fig. 18(b) supported the cell viability upon incubation onto the repellent formulation 2.

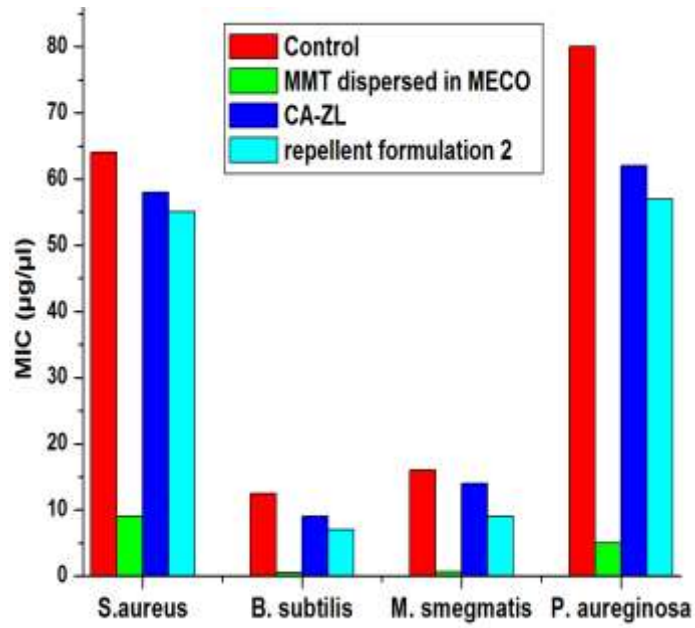


**Fig. 17.** Antibacterial efficacy of MMT dispersed in MECO, ZL-CA oil extract and the repellent formulation 2.

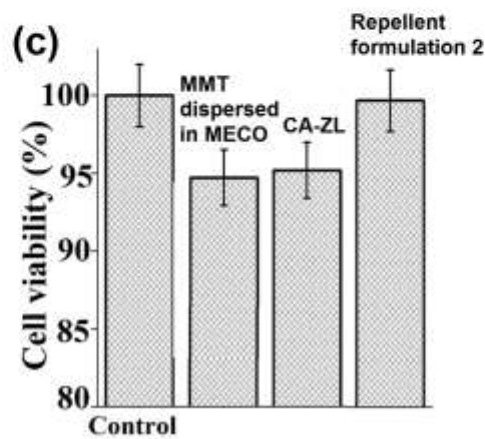
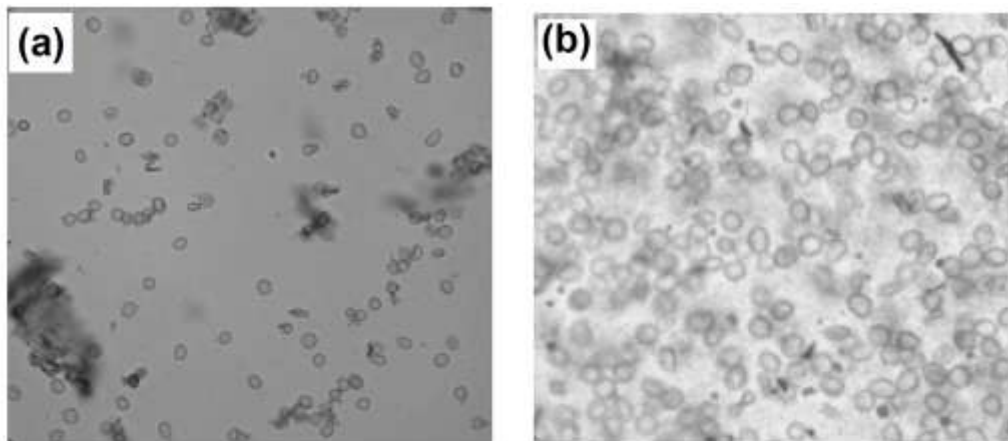


**Fig. 18.** Biocompatibility in terms of Typhan blue assay of (a) control and, (b) repellent formulation 2, and (c) MTT assay.

#### 4. CONCLUSION

The HBPEA/PAni nanofiber nanocomposite was successfully prepared and characterized. The application of the green chemistry tool namely sonication was explored to efficiently immobilize the DRL herbal formulation onto the nanomaterials. The immobilized nanofibers are characterized using UV-Visible and FTIR spectroscopic tools. The controlled release of the herbal formulation from the immobilized nanofiber at different temperature showed that the release profile was in controlled manner as a function of time and temperature. However the low mosquito repellent efficiency of the nanocomposite system compelled us to study the immobilization of CA-ZL essential oil mixture onto MMT dispersed in an environmentally benign solvent of MECO. This repellent formulation 2 gave pronounced repellent activity. The above study successfully fabricated an efficient repellent formulation containing 3:2 wt% CA-ZL immobilized onto MMT dispersed in MECO. Thus the fabrication of the repellent system 2 is envisaged to pursue future commercialization as potent vaporizer technology.

**DELIVERABLE/OUTCOME:** *A formulation containing 3:2 wt% CA-ZL immobilized onto MMT dispersed in MECO with prolong mosquitoes repellency and acceptable activity was formulated.*

## REFERENCE

1. Rao TR, Dhanda V, Bhat HR, Kulkarni SM, *The Indian Journal of Medical Research*, 61, 1421-1461, 1973.
2. Rattanarithikul R, Panthusiri P, *The Southeast Asian Journal of Tropical Medicine and Public Health*, 25, 1-66, 1994.
3. Weldon PJ, Klun JA, Oliver JE, Debboun M, *Naturwissenschaften*, 90, 301-304, 2003.
4. Agyepong IA, Manderson L, *Journal of Biosocial Science*, 31, 79-92, 1999.
5. Amer A, Mehlhorn H, *Parasitology Research*, 99, 478-490, 2006.
6. Madhu SK, Shaukath AK, Vijayan VA, *Acta Tropica*, 113, 7-11, 2010.
7. Maji TK, Baruah I, Dube S, Hussain, MR, *Biores Technol*, 98, 840-844, 2007.
8. Nerio LS, Olivero-Verbel J, Stashenko E, *Biores Technol*, 101, 372-378, 2010.
9. Balzani V, *Small*, 1, 278-283, 2005.
10. Panella B, Hirscher M, Roth S, *Carbon*, 43, 2209-2214, 2005.
11. Huang J, Kaner RB, *J. Am. Chem. Soc.* 126, 851-855, 2004.
12. Brindley GW, Ray S, *Am Mineral*, 49, 106-115, 1964.
13. Mahapatra SS, Karak N, *Prog Org Coat*, 51, 103-108, 2004.
14. Xia Y, Larock RC, *Green Chem*, 12, 1893-1909, 2010.
15. Ogunniyi DS, *Biores Technol*, 97, 1086-1091, 2006.
16. Meneghetti SMP, et al. *Energ Fuel*, 20, 2262-2265, 2006.
17. Radhika P, et al. *Res J Biotech*, 3, 62-63, 2008.
18. Niu Q, et al. *J Immunol Methods*, 251, 11-19, 2001.
19. Owen GR, *Eur Cells Mater*, 9, 85-96, 2005.
20. Shende P, et al. *Pigment & Resin Technology*, 32, 4-9, 2003.
21. Ahmad S, et al. *J Appl Polym Sci*, 104, 1143-1148, 2007.
22. Shende PG, et al. *Pigment & Resin Technology*, 31, 310-314, 2002.
23. Meshram PD, et al. *Prog Org Coat*, 76, 1144-1150, 2013.
24. Bharathi NP, et al. *J Inorg Organomet Polym*, 20, 839-846, 2010.
25. Ahmad S, et al. *J Polym Mater*, 18, 53-60, 2001.
26. Ahmad S, et al. *Prog Org Coat*, 47, 95-102, 2003.
27. Kelland MA, *J Appl Polym Sci*, 121, 2282-2290, 2011.
28. Oguntimein BO, et al. *Flavour and Fragrance Journal*, 5, 89-90, 1990.
29. Itthipanichpong C, Ruangrunsi N, Pattanaautsahakit C, *Journal of the Medical Association of Thailand*, 85, S344-54, 2002.
30. Banerjee S, et al. *Nanotechnology*, 21, 045101, 2010.

## LIST OF PUBLICATIONS

1. S. Pramanik, N. Karak, S. Banerjee, A. Kumar, Effects of solvent interactions on the structure and property of prepared PANi nanofibers, *J. Appl. Polym. Sci.* 126(2012)830-836
2. S. Pramanik, K. Sagar, B. K. Konwar and N Karak, Synthesis, characterization and properties of a castor oil modified biodegradable poly(ester amide) resin, *Prog. Org. Coat.* 75(2012)569-578.
3. S. Pramanik, R. Konwarh, K. Sagar, B. K. Konwar and N Karak, Bio-degradable vegetable oil based hyperbranched poly(ester amide) as an advanced surface coating material, *Prog. Org. Coat.* 76(2013)689-697.
4. S. Pramanik, J. Hazarika, A. Kumar, and N. Karak, Castor oil based hyperbranched poly(ester amide)/polyaniline nanofiber nanocomposites as antistatic materials, *Ind. Eng. Chem. Res.* 52(2013)5700–5707.

## FINAL AUDITED UTILIZATION CERTIFICATE FOR THE PERIOD 01.04.13 TO 31.03.14

1. Title of the Project: "STUDIES ON GREEN POLYMERIC NANOCOMPOSITES FOR DEVELOPMENT OF INSECT REPELLANT FORMULATIONS".

2. Name of the Institution: TEZPUR UNIVERSITY

3. Principal Investigator: PROF. NIRANJAN KARAK

4. DRL letter No. and date sanctioning the project: DRL/1047/TC, dated 2<sup>nd</sup> March 2011.

5. Head of account as given in the original sanction letter: For 2<sup>nd</sup> year

Sanctioned Heads	Funds allotted (Rs.)
Research Staff	1,20,000/-
Equipment ( including spares thereof)	-
Operation and Maintenance of equipment	-
Expendables (Consumable Stores)	30,000/-
Travel	-
Contingencies	20,000/-
Visiting faculties	-
Procured services	-
Institutional overheads	8, 500/-
Column Total	1,78,500/-

6. Amount brought forward from the previous Financial year quoting DRL letter No. and date in which the authority to carry forward the said amount is given

i. Amount: Rs. 12,113/-  
ii. Letter No.: DRL/1047/TC  
iii. Date: 02.03.11

7. Amount received during the financial year:

i. Amount: Rs. 1,78,500/-  
ii. Letter No.: DIH-116(DRL-A5)  
iii. Date: 01.07.13

8. Total amount that was available for expenditure (excluding commitments) during the financial year (S. No. 6 + 7):

Rs. 1,90,613/-

9. Actual expenditure (excluding commitments) incurred during the 01.04.11 to 31.03.12:

Rs. 1,45,758/-

10. Balance amount available at the end of the 3<sup>rd</sup> year:

Rs. 44,855/-

11. Unspent balance refunded, if any:

Rs. 44,405/- \*

\* Actual balance is Rs.(44,855-450)/- = Rs.44,405/-, as excess receipt shown in the first year (2011-2012) grant is Rs.(598450-598000)/- = Rs. 450/-.

12. Amount to be carried forward to the next year:

Nil



तेजपुर विश्वविद्यालय

(केन्द्रीय विश्वविद्यालय)

नपाम, तेजपुर - 784 028, असम, भारत

TEZPUR UNIVERSITY

( A Central University)

Napam, Tezpur - 784 028, Assam, India

**AUDITED UTILISATION CERTIFICATE**

Certified that out of **Rs. 1,78,500/-** of grants-in-aid sanctioned during the year **2013-2014** in favor of Registrar, Tezpur University under this Ministry of Defence order No **DIH-116(DRL-AS)** dated **1<sup>st</sup> July 2013** and **Rs. 12,113/-** on account of unspent balance of the previous year, a sum of **Rs. 1,45,758/-** has been utilized for the purpose of project for which it was sanctioned. The balance of **Rs. 44,405/-** remaining unutilized at the end of **31<sup>st</sup> March 2014** is refunded vide bank draft No. **895067** dated **13/06/2014**.

 Prof. N. Karak Principal Investigator <b>Dr. Niranjana Karak</b> Date: <b>12/05/14</b> Professor Department of Chemical Sciences Tezpur University	 Finance Officer Tezpur University Date: <b>Finance Officer</b> Tezpur University	 Registrar Tezpur University Date: <b>Registrar</b> Tezpur University	For <b>SURAJIT CHAKRABORTY &amp; CO.</b> CHARTERED ACCOUNTANTS  CA. <b>SURAJIT CHAKRABORTY</b> Auditor (Proprietor) Membership No. - 305054 Date:
---	---	--	--

(TO BE FILLED IN DRL)

Certified that I have satisfied myself that the conditions on which the grants in aid was sanctioned have been fulfilled/are being fulfilled and that I have exercised the necessary checks to see that the money was actually utilized for the purpose for which it was sanctioned.

Signature

Designation:

Date:

**FINAL AUDITED STATEMENT OF EXPENDITURE ACCOUNTS FOR THE FINANCIAL YEAR FROM 01 APRIL 2013 TO 31 MARCH 2014**

Title of the project: "STUDIES ON GREEN POLYMERIC NANOCOMPOSITES FOR DEVELOPMENT OF INSECT REPELLANT FORMULATIONS".

- (a) Sanction letter No.: DRL/1047/TC, dated 2<sup>nd</sup> March 2011.  
 (b) Principal Investigator: PROF. NIRANJAN KARAK  
 (c) Total sanctioned Cost of the Project: 9,55,500 INR  
 (d) Grant received in 1<sup>st</sup> & 2<sup>nd</sup> yr: 11 yr. - Rs. 12,11,13/- (unspent from 2<sup>nd</sup> installment) + Rs. 1,78,500/- (as 3<sup>rd</sup> installment). Total - Rs. 1,90,613/-.

S. No	Sanctioned Heads	Funds allotted for the year 2013-14	Funds released	Carried forward from previous year (2012-13)	Funds Available (iv + v)	Expenditure incurred during the financial year 2013-14	Balance* (vi - vii)	Commitments	Total expenditure (vii + ix)
		ii	iii	iv	v	vi	vii	ix	x
(a)	Research Staff	1,30,000/-	1,30,000/-	-	1,30,000/-	80,000/-	40,000/-	-	80,000/-
(b)	Specific Equipment (including spares thereof)	-	-	12,010/-	12,010/-	7,272/-	4,738/-	-	7,272/-
(c)	Operation and Maintenance of equipment	-	-	-	-	-	-	-	-
(d)	Expendables (Consumable Stores)	30,000/-	30,000/-	103/-	30,103/-	30,000/-	103/-	-	30,000/-
(e)	Travel (T/A / DA)	-	-	-	-	-	-	-	-
(f)	Contingencies	20,000/-	20,000/-	-	20,000/-	19,986/-	14/-	-	19,986/-
(g)	Visiting faculties	-	-	-	-	-	-	-	-
(h)	Professional services	-	-	-	-	-	-	-	-
(i)	Institutional overheads	8,500/-	8,500/-	-	8,500/-	8,500/-	nil	-	8,500/-
	Column Total	1,78,500/-	1,78,500/-	12,113/-	1,90,613/-	1,45,758/-	44,855/-	-	1,45,758/-

\*Actual balance is Rs. (44,855-450/-) = Rs. 44,405/-, as excess receipt shown in the first year (2011-2012) grant is Rs. (598450-598000)/- = Rs. 450/-.  
 Therefore an amount of Rs. 44,405/- is refunded against draft in favor of Director DRL, Tezpur to the funding agent.

*Niranjan Karak*  
 Prof. Karak  
**Dr. Niranjan Karak**  
 Professor

Department of Chemical Sciences  
 Tezpur University

*B. Dwivedi*  
 Finance Officer  
 S.O.14  
 Tezpur University

Finance Officer  
 Tezpur University

*Pranav*  
 Registrar  
 Tezpur University

Registrar  
 Tezpur University

**For SURAJIT CHAKRABORTY & CO.**  
 CHARTERED ACCOUNTANTS  
*Surajit Chakraborty*  
 Auditor  
**CA SURAJIT CHAKRABORTY**  
 (Proprietor)  
 Membership No.: 302054  
 Date: 16/05/14